

Effects of Low Pressure Injection on Fuel Atomization and Mixture Formation for Heavy Fuel Engines

Authors:

Rui Liu, Kaisheng Huang, Yuan Qiao, Haocheng Ji, Lingfeng Zhong, Hao Wu

Date Submitted: 2023-02-21

Keywords: HFE, two-stroke, injection control, air-assisted atomization, fuel–air mixture

Abstract:

The application of direct injection (DI) technology can effectively improve the atomization effect of heavy fuel to reduce the fuel loss of heavy fuel engines (HFE). The fuel spray characteristics directly affect the combustion performance of the engine. To investigate the atomization process and evaporation characteristics of heavy fuel in-cylinder for an air-assisted direct injection (AADI) engine, a simulation calculation model of AADI HFE was established with the use of a computational fluid dynamics tool. The air-assisted injector model and the one-dimensional performance calculation model were verified by test data. The influences of injection timing and injection pressure on the spray characteristics and mixture formation in the engine cylinder were discussed. The results show that the mixture concentration distribution is uniform after the injection timing is advanced, and the mass fraction of the fuel evaporation increases. The earlier injection timing can provide the fuel with sufficient time to evaporate, while the later injection timing will result in increasing the Sauter mean diameter (SMD) of the fuel droplets, and the unevaporated heavy fuel in the combustion chamber tends to become concentrated. With the increase in air injection pressure, the distribution of the mixed gas in the cylinder becomes uniform, and the SMD of the fuel droplets in the cylinder decreases. When the injection pressure is 0.65 MPa and 0.75 MPa, the difference between the SMD of the fuel droplets in-cylinder decreases, and a favorable fuel atomization effect can be maintained.

Record Type: Published Article

Submitted To: LAPSE (Living Archive for Process Systems Engineering)

Citation (overall record, always the latest version):

LAPSE:2023.0808

Citation (this specific file, latest version):

LAPSE:2023.0808-1

Citation (this specific file, this version):

LAPSE:2023.0808-1v1

DOI of Published Version: <https://doi.org/10.3390/pr10112276>

License: Creative Commons Attribution 4.0 International (CC BY 4.0)

Article

Effects of Low Pressure Injection on Fuel Atomization and Mixture Formation for Heavy Fuel Engines

Rui Liu ^{1,2} , Kaisheng Huang ^{1,*} , Yuan Qiao ¹, Haocheng Ji ², Lingfeng Zhong ² and Hao Wu ³¹ State Key Laboratory of Automotive Safety and Energy, Tsinghua University, Beijing 100084, China² School of Mechanical and Power Engineering, Nanjing Tech University, Nanjing 211816, China³ Nanjing Changkong Technology Co., Ltd., Nanjing 211106, China

* Correspondence: huangks@tsinghua.edu.cn

Abstract: The application of direct injection (DI) technology can effectively improve the atomization effect of heavy fuel to reduce the fuel loss of heavy fuel engines (HFE). The fuel spray characteristics directly affect the combustion performance of the engine. To investigate the atomization process and evaporation characteristics of heavy fuel in-cylinder for an air-assisted direct injection (AADI) engine, a simulation calculation model of AADI HFE was established with the use of a computational fluid dynamics tool. The air-assisted injector model and the one-dimensional performance calculation model were verified by test data. The influences of injection timing and injection pressure on the spray characteristics and mixture formation in the engine cylinder were discussed. The results show that the mixture concentration distribution is uniform after the injection timing is advanced, and the mass fraction of the fuel evaporation increases. The earlier injection timing can provide the fuel with sufficient time to evaporate, while the later injection timing will result in increasing the Sauter mean diameter (SMD) of the fuel droplets, and the unevaporated heavy fuel in the combustion chamber tends to become concentrated. With the increase in air injection pressure, the distribution of the mixed gas in the cylinder becomes uniform, and the SMD of the fuel droplets in the cylinder decreases. When the injection pressure is 0.65 MPa and 0.75 MPa, the difference between the SMD of the fuel droplets in-cylinder decreases, and a favorable fuel atomization effect can be maintained.

Keywords: HFE; two-stroke; injection control; air-assisted atomization; fuel–air mixture



Citation: Liu, R.; Huang, K.; Qiao, Y.; Ji, H.; Zhong, L.; Wu, H. Effects of Low Pressure Injection on Fuel Atomization and Mixture Formation for Heavy Fuel Engines. *Processes* **2022**, *10*, 2276. <https://doi.org/10.3390/pr10112276>

Academic Editors: Dezhi Zhou and Jing Li

Received: 16 September 2022

Accepted: 31 October 2022

Published: 3 November 2022

Publisher's Note: MDPI stays neutral with regard to jurisdictional claims in published maps and institutional affiliations.



Copyright: © 2022 by the authors. Licensee MDPI, Basel, Switzerland. This article is an open access article distributed under the terms and conditions of the Creative Commons Attribution (CC BY) license (<https://creativecommons.org/licenses/by/4.0/>).

1. Introduction

Aviation piston engines have the characteristics of low manufacturing and maintenance costs, high power-to-weight ratio, and strong compatibility, which make them widely used in the field of small aviation power plants [1–3]. Typical aviation piston engines mainly use gasoline, with favorable evaporation and ignitability, as the fuel. Heavy fuel (light diesel and aviation kerosene) has a high flash point, and the fuel is safer in the processes of storage, transportation, and usage [4,5]. Heavy fuel has high viscosity and favorable stability, and its atomization effect is weaker than that of ordinary gasoline under the same conditions. When the traditional two-stroke aviation piston engine burns heavy fuel, the injected fuel droplets will easily condense into fuel film when they meet the cold wall, and the evaporation process of fuel film is slower than that of gasoline [6,7]. In recent years, the DI technology of heavy fuel has attracted much attention. The application of DI technology can effectively improve the atomization effect of heavy fuel, reduce the fuel loss of the heavy fuel aviation piston engine, and improve engine performance. Direct injectors are divided into different types, including high pressure swirl injectors, slit injectors, shaped injectors, and air-assisted injectors. Among these, as one of the types of gas-assisted injectors, low-pressure air-assisted injectors are usually used for power systems such as small-scale fuel-powered unmanned aerial vehicles, motorcycles, and off-board machines, showing favorable atomization performance and remarkable fuel saving effects.

In the application case of a two-stroke or four-stroke DI spark-ignition (SI) HFE, the fuel spray characteristics directly affect the combustion performance of the engine [8,9]. Chen et al. [10] calibrated a simulation model using test data from a DISI engine to investigate the behavior of diesel combustion. Their research indicates that diesel combustion is slower compared to that of gasoline, and the knock tendency is higher. For a diesel–air mixture with equivalence ratios of 0.6 to 1.4, higher combustion pressure and faster burning rate occur when the equivalence ratios are 1.2 and 1.0; however, the latter has a higher knock possibility. Moreover, they also established a combustion model of the two-stroke engine to study the heavy-fuel combustion at different ignition timings and equivalence ratios. The results show that aviation kerosene is less prone to knock than diesel and can achieve better combustion performance under the condition of rich mixture [11]. Zhao et al. [12] studied the air scavenging and mixture formation process of a two-stroke DISI engine fueled with kerosene. Postponing fuel injection reduces the short-circuit time of fuel and avoids the free exhaust phase with large exhaust mass flow, which can improve the fuel capture rate. Late injection will result in incomplete evaporation and the uneven mixture of fuel and air. In addition, the formation process of the mixture in-cylinder of a two-stroke ignition HFE was simulated by Huang [13]. The ideal mixing distribution can be formed in the whole working condition range through the mutual organization and coordination of fuel injection control and in-cylinder air flow. Wang et al. [14,15] calculated the gas-phase flow field and spray field as kerosene and gasoline fuel were injected into the constant-volume chamber at different inlet pressures under the condition that the needle valve was fully open. The simulation results indicate the influence of the change in the gas-phase pressure ratio of the Laval nozzle on the penetration distance, SMD, and particle size distribution of air-assisted atomization. Ji et al. [16] numerically analyze the process of air-assisted atomization for diesel spray. Their calculation model considering the diesel injection process in the fuel–air premixing chamber was established without changing the injector structure. The air-assisted injection process of diesel–air two-phase flow was investigated in a constant volume chamber. The effects of air injection pressure, ambient back pressure, and fuel temperature on diesel spray characteristics were investigated, revealing great theoretical reference significance. In summary, the traditional SI HFEs produce a homogeneous fuel mixture by means of port injection such that the fuel control strategy is simplified. With the application of air-assisted atomization in the DISI HFEs, the whole spray size of the fuel droplets is greatly reduced, which is of great significance in promoting stable fuel–air mixing and combustion.

In this paper, an improved three-dimensional calculation model will be established based on low pressure air-assisted atomization injection. For this model, the needle valve lift will be given according to the experimental measured data. The dynamic mesh method will be used to simulate the transient spray field of the direct injector in the engine cylinder when the needle valve moves. The influence of the control parameters, including the injection pressure and the injection timing, on the spray characteristics of the air-assisted injector will be evaluated, and the SMD at different crankshaft positions after injection will be statistically analyzed. The droplet size of the fuel spray in the engine cylinder and the distribution characteristics of the fuel–air mixture will be investigated.

2. Modeling and Settings

2.1. Meshing of the Three-Dimensional Calculation Model

With the help of the ICEM tool, the three-dimensional calculation meshing model for the DI HFE is given. The size of the air-assisted direct injector, the scavenging port, the combustion chamber, and the exhaust port are defined, respectively. The meshing model file required for the three-dimensional numerical simulation calculation is generated after completing each division and process for these ports. The meshing model is then imported into the workbench of FLUENT to perform the calculation routine. Figure 1 shows the three-dimensional structural model of the engine and its meshing model for

all computational domains. It is worth noting that the meshes at the junctions of the air-assisted injector, outlets of the scavenging port, and inlet of the exhaust port are refined.

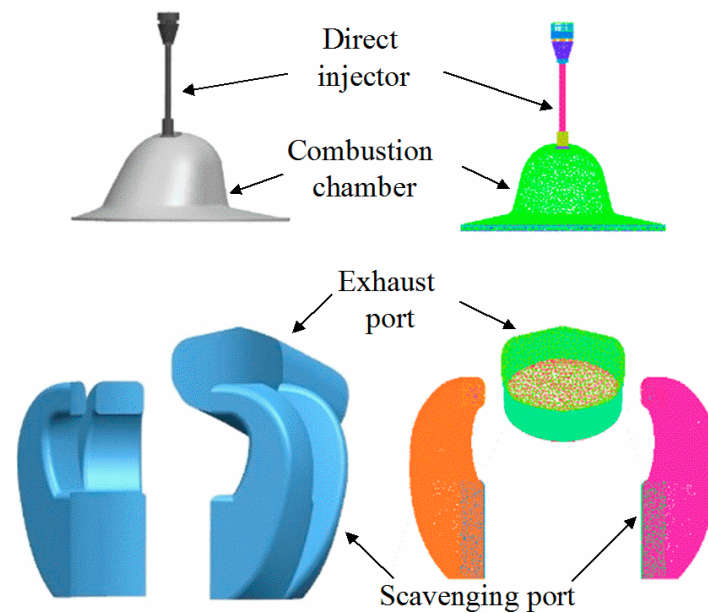


Figure 1. Three-dimensional engine model and meshing model of computational domains.

2.2. Dynamic Mesh

In order to truly simulate the operational state of the engine, it is necessary to set the dynamic mesh reflecting the piston operation and the opening and closing process of the needle valve in the calculation model. For the whole simulation process for fuel spray in the engine cylinder and combustion chamber, the piston motion must cover a single complete working cycle; that is, the crankshaft rotation period must be at least 360°CA ($^\circ\text{CA}$ refers to crankshaft angle). Figure 2 shows the dynamic meshes of the piston and cylinder wall in the engine fluid domains under three crankshaft positions (TDC refers to top dead center, BTDC refers to before TDC, and ATDC refers to after TDC). Figure 3 shows the needle valve dynamic mesh of the air-assisted direct injector.

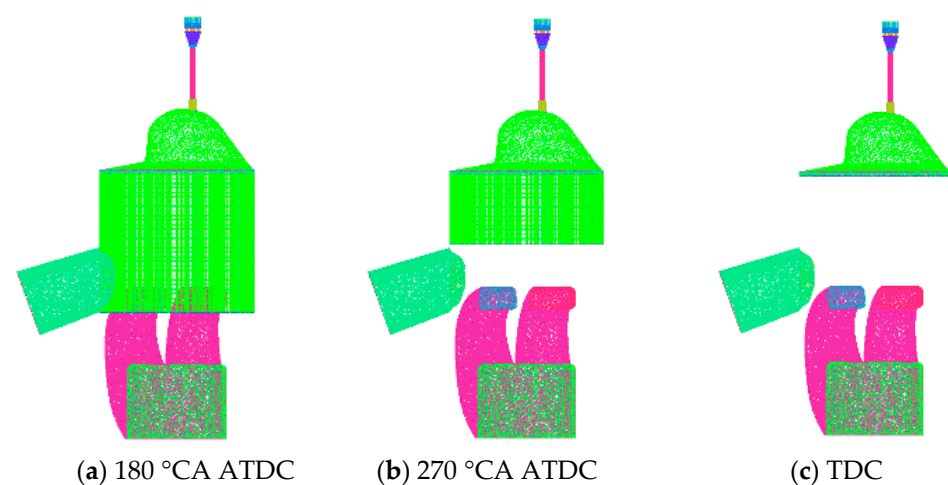


Figure 2. Dynamic meshes of the piston and cylinder wall in the engine fluid domains.

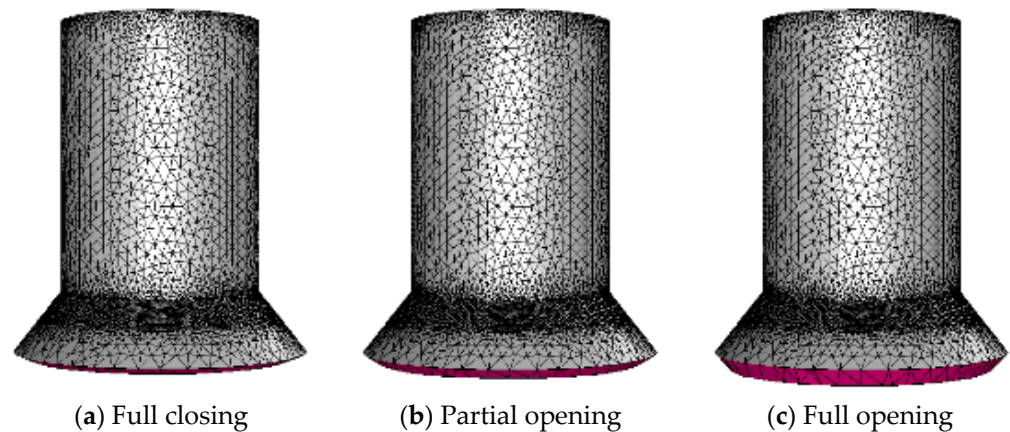


Figure 3. Dynamic mesh of the needle valve for the air-assisted injector.

2.3. Injector Model

The premixed process for fuel and compressed air realized by an air-assisted direct injector is a typical two-phase flow problem. The fluid phase is treated as a continuous phase by the Lagrange method, and the fuel droplets are treated as discrete phases and are distributed in the continuous phase. The realizable k - ε turbulence model, which is improved on the basis of the standard k - ε model, was selected for the spray calculation model [17]. This model adds a constraint formula for turbulent viscosity and a transmission equation for the dissipation rate, which can better realize rotary flow, flow separation, and complex secondary flow. Turbulent kinetic energy k and turbulent dissipation rate ε in the model transport equation are as follows:

$$\frac{\partial}{\partial t}(\rho k) + \frac{\partial}{\partial x_i}(\rho k u_i) = \frac{\partial}{\partial x_i} \left[\left(\mu + \frac{\mu_t}{\sigma_k} \right) \frac{\partial k}{\partial x_i} \right] + G_k + G_b - \rho \varepsilon - Y_M + S_k \quad (1)$$

$$\frac{\partial}{\partial t}(\rho \varepsilon) + \frac{\partial}{\partial x_i}(\rho \varepsilon u_i) = \frac{\partial}{\partial x_i} \left[\left(\mu + \frac{\mu_t}{\sigma_\varepsilon} \right) \frac{\partial \varepsilon}{\partial x_i} \right] + \rho C_1 S_\varepsilon - \rho C_2 \frac{\varepsilon^2}{k + \sqrt{\nu \varepsilon}} + C_{1\varepsilon} \frac{\varepsilon}{k} C_{3\varepsilon} G_b + S_\varepsilon \quad (2)$$

In Equation (1), σ_k equals 1.0; μ_t is the turbulent viscosity; ρ is the gas density; G_k represents the turbulent kinetic energy due to the average velocity gradient; G_b is the turbulent kinetic energy due to buoyancy; Y_M represents the contribution of fluctuation expansion in compressible turbulence to the total dissipation rate; S_k is a custom source item. In Equation (2), σ_ε equals 1.2; C_2 equals 1.9; $C_{1\varepsilon}$ equals 1.44; other relevant parameters can be calculated by referring to the references [17].

The TAB (Taylor analogy breakup) model is selected as the droplet breakup model. Based on the theory of elastic mechanics, the breakup process of oscillating droplets is compared with the vibration of the spring damping system. The mass block is subjected to external force similar to the droplet and is also subjected to aerodynamic force. The spring elastic force is similar to the surface tension of the droplet, and the damping is similar to the viscosity of the liquid [18]. The calculation formula is as follows:

$$\ddot{y} = \frac{C_F \rho_g u^2}{C_b \rho_l r^2} - \frac{C_k \sigma}{\rho_l r^3} y - \frac{C_d \mu_l}{\rho_l r^2} \dot{y} \quad (3)$$

In Equation (3), y is the dimensionless deformation of droplet maximum diameter; ρ_g is the gas density; ρ_l is the liquid density; u is the relative velocity of the gas and the droplet; r is the droplet radius; C_F , C_k , C_d , and C_b are the dimensionless constants determined by mathematical analysis and the experiments.

The initial droplet will oscillate normally in the spray process. If the deformation is affected by aerodynamic force and exceeds a certain value; that is, $y > 1$, the initial droplet will break up and produce smaller secondary droplets. The normal velocity of the secondary

droplet is equal to the normal oscillation velocity of the initial droplet when the droplet breaks, so the cone angle of the spray can be calculated automatically by the model. The SMD (r_{32}) of sub-droplets can be calculated by the following energy conservation equation:

$$\frac{r}{r_{32}} = 1 + \frac{8 \cdot K}{20} + \frac{\rho_1 r^3}{\sigma} \dot{\gamma}^2 \left(\frac{6 \cdot K - 5}{120} \right) \quad (4)$$

K is used to adjust the size ratio of the initial droplet to the secondary droplet. The larger the value, the smaller the size of the broken droplet.

In addition, after droplet evaporation, the flow field medium contains multiple components, and the following component transport equation needs to be solved:

$$\frac{\partial}{\partial t}(\rho Y_i) + \nabla \cdot (\rho \bar{v} Y_i) = -\nabla \bar{J}_i + R_i + S_i \quad (5)$$

where Y_i represents the mass fraction of each component, S_i is the original, \bar{J}_i is the diffusion flux caused by the concentration gradient, and R_i is the net production rate of the chemical reaction [19].

The R-R (Rosin–Rammler) model is selected for droplet size distribution.

$$R(D) = 100 \exp[-(D/D_e)^n] (\%) \quad (6)$$

where $R(D)$ represents the cumulative mass percentage of sieve corresponding to droplet size D ; when $D = D_e$, the cumulative mass percentage of sieve $R(D_e) = 100 / e \% = 0.368$, and the corresponding droplet size is the characteristic particle size D_e of the particle group, which can roughly reflect the thickness of the fuel droplet. n is the uniformity coefficient, which is used to characterize the range of droplet distribution [20].

The definition of SMD is as follows:

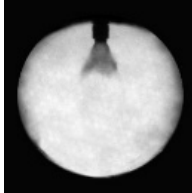
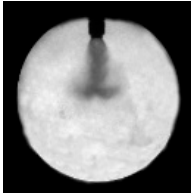
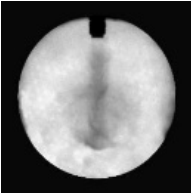
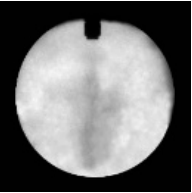
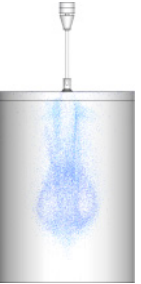
$$\text{SMD} = \frac{\sum N_i d_i^3}{\sum N_i d_i^2} \quad (7)$$

where N represents the number of droplets, d represents the diameter of the droplets, and the physical meaning of SMD is the corresponding diameter after converting the cube into an equal volume sphere.

The direct injector assembly includes three parts: fuel injector, premixing chamber, and air-assisted injector. The gaseous medium is air. To simulate the entire process that conforms with the actual scenario, fuel is first ejected through the outlet of fuel injector to the premixing chamber and then delivered by air-assisted injector into the constant volume chamber or engine cylinder. In order to verify the simulation model for AADI, the calculation results are analyzed according to the injection process of the air-assisted injector. The fuel spray characteristics obtained by a high-speed photography experimental system and the simulation calculation are compared. Table 1 shows the high-speed spray images and the spray simulation images at different times during the opening process of the needle valve under the conditions of 6.5 bar air injection pressure and 0 bar ambient pressure (gauge pressure). The fuel used is light diesel, and the fuel properties can be obtained in the reference [21]. Figure 4 shows the comparison results of the spray characteristic parameters between the experimental measurement and the simulation calculation. It can be seen from the figure that the penetration distance measured by the experiment is slightly larger than that of the simulation calculation value. This is mainly due to the fact that the fuel injection rate used in the simulation is the average rate, which has a certain influence on the spray change. Overall, the ratio of fuel SMD to penetration distance is basically consistent, and the calculation results from the simulation model are close to those of the actual situation. Therefore, the results can lay the foundation for the calculation and analysis of the fuel spray characteristics and mixture formation process in the engine cylinder under

different air injection pressures, injection timings, and other injection parameters in the subsequent sections.

Table 1. Comparison of fuel spray tests and calculation results.

Injection Time	1 ms	2 ms	3 ms	4 ms
Test				
Calculation				

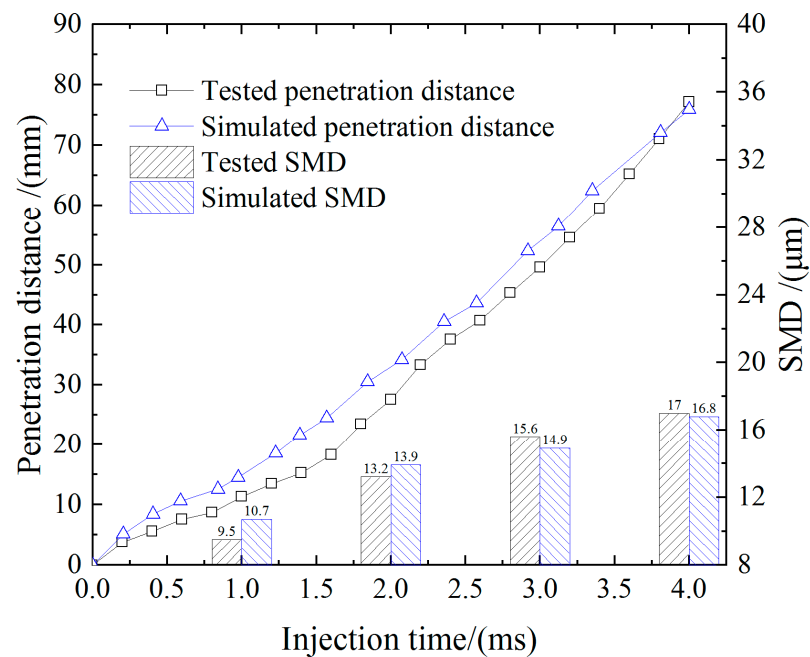


Figure 4. Comparisons of spray characteristics between the test and simulation.

2.4. Initial Conditions and Boundary Conditions

The specific technical parameters of the AADI SI HFE are listed in the reference [22]. According to the structure of the test engine, one-dimensional modeling can be divided into intake and exhaust systems, fuel injection systems, cylinders, and crank linkages [23]. A one-dimensional simulation model of the engine, established by selecting the corresponding module in GT-Power, is shown in Figure 5. In order to ensure the accuracy of the one-dimensional performance calculation simulation model, it is necessary to check the simulation results of the established model with the bench test data. In this study, the engine power for the one-dimensional model is calibrated. The throttle opening, rotational speed, excess air coefficient, and ignition timing angle used in the bench test are input

into the corresponding module, and a set of combustion parameters consistent with the power under the test conditions are obtained by repeatedly calculating and adjusting the combustion parameters for the in-cylinder module [24]. Figure 6a shows the power comparison results of the calculated values from this model and the test values at conditions of an engine speed of 4000 r/min and different throttle opening positions. At the same time, taking the full load operation point as an example, Figure 6b shows the cylinder pressure verification results of the test and simulation under full load. The resulting errors between the simulation and the test are within 5%, which verifies the accuracy and rationality of the one-dimensional calculation model.

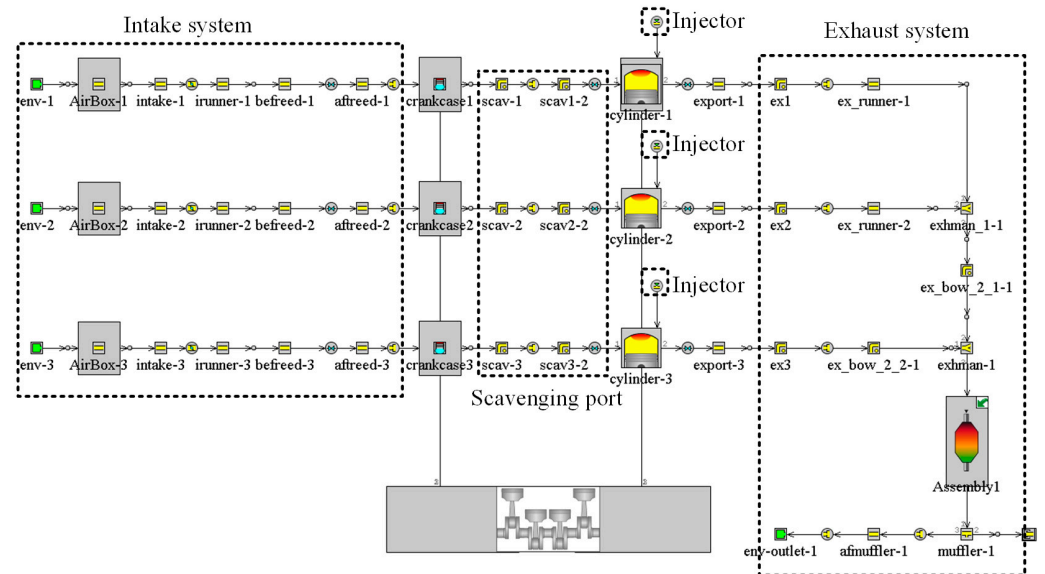


Figure 5. One-dimensional performance calculation model for the test engine.

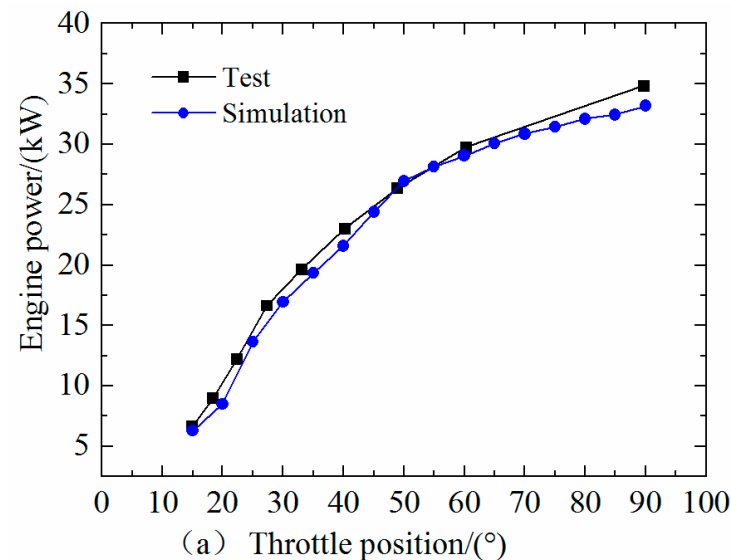


Figure 6. Cont.

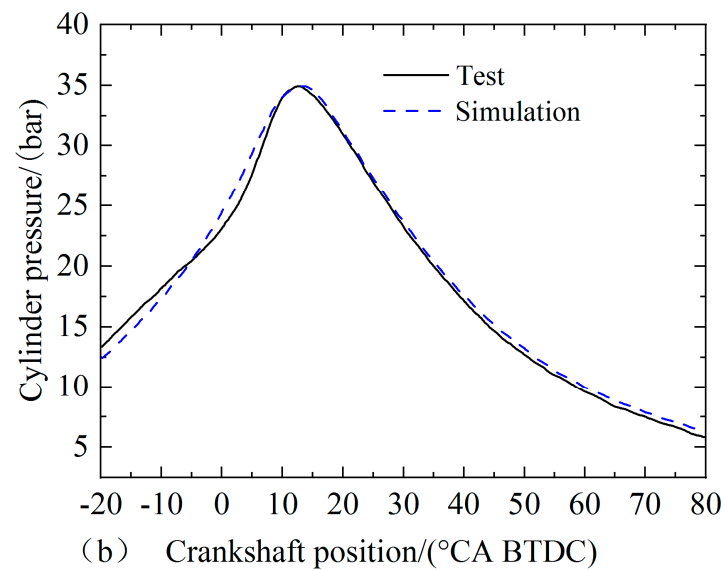


Figure 6. Validation of the calculation model with the test data: (a) engine output; (b) combustion pressure.

In the three-dimensional numerical simulation, the initial conditions are based on the bench test data, while the boundary conditions must be set in the calculation case for this calculation model. All the required boundary pressure parameters for the three-dimensional numerical simulation can be obtained according to the calibrated one-dimensional performance simulation model, as described in the reference [25]; Figures 5 and 6 provide the basis for boundary pressure calculation. As shown in Figure 7, the crankcase pressure and exhaust pressure are calculated through the calibrated one-dimensional simulation model under the condition of an engine speed of 4000 r/min and a partial load. Therefore, according to this group of data, the crankcase pressure can be set as the inlet pressure of the scavenging port in the three-dimensional model, and the transient exhaust pressure can be set as the outlet pressure.

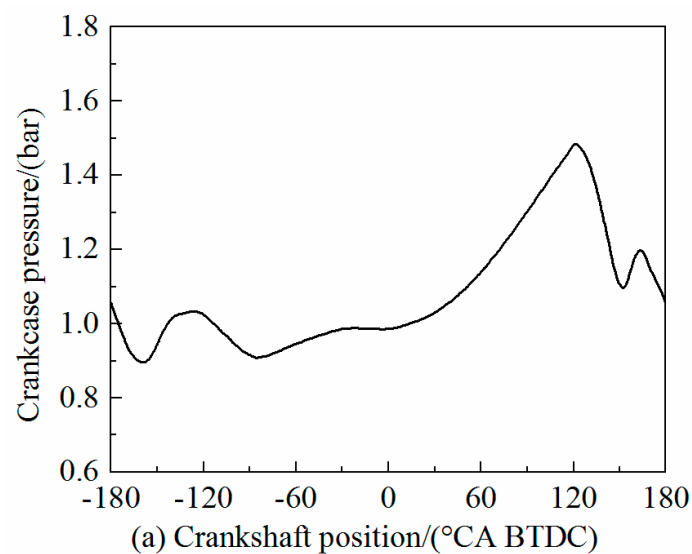


Figure 7. Cont.

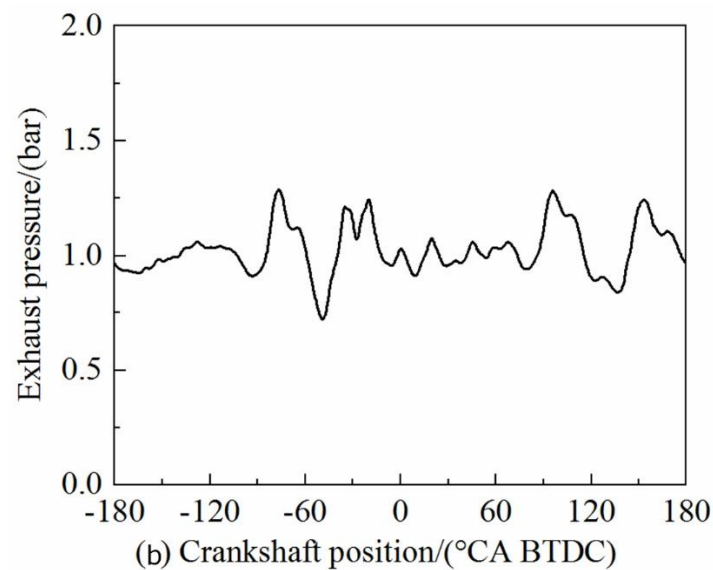


Figure 7. Boundary conditions for pressure inlet and outlet: (a) crankcase pressure; (b) exhaust pressure.

3. Heavy Fuel Atomization and Mixture Formation Analysis

Under the condition of partial loads, the throttle opening is limited, and the air intake locates at a low level. The corresponding engine heat load during the operation is relatively small. The evaporation characteristics of heavy fuel in-cylinder are sensitive to the control of injection parameters, and the distribution of a combustible mixture will also be affected accordingly. In this section, the simulation calculation for the formation of fuel spray and the mixture in-cylinder is carried out for the condition of a partial load at an engine speed of 4000 r/min. The fuel material is light diesel. Adjusting the injection timing and injection pressure to obtain the fuel–air mixture concentration in-cylinder at different crankshaft positions, the distribution law of a fuel–air mixture is analyzed.

3.1. Effects of Injection Timing on Fuel Atomization and Mixture Formation

To analyze the influence of injection timing on the fuel atomization characteristics and mixture distribution characteristics in the engine cylinder, Figure 8 shows the fuel–air mixture concentration distribution at the crankshaft positions from 330 °CA ATDC to TDC with the engine speed of 4000 r/min. The injection timings (start of injection) are 126 °CA BTDC, 176 °CA BTDC and 226 °CA BTDC, respectively. For these calculation cases, the injection pressure is 6.5 bar and the fuel temperature is 293 K. The injection timing of 126 °CA BTDC presents the late fuel injection strategy. It can be observed from the figure that as the engine crankshaft position is 340 °CA ATDC, the air–fuel ratios around the spark plugs installed at the intake side and exhaust side are about 23.7. Therefore, the fuel–air mixture concentration is relatively thin, which indicates the injection timing is too late. The comprehensible reason is that as the fuel spray is injected with late timing, the ambient pressure in the engine combustion chamber is relatively high, and most of the fuel droplets gather at the top of the combustion chamber. In addition, the insufficient evaporation time for the fuel droplets makes the formation of the fuel–air mixture inhomogeneous in the combustion chamber, and the distribution area is small. As the injection timings are advanced from 176 °CA BTDC to 226 °CA BTDC, the mass fraction of evaporated fuel in the engine cylinder increases gradually. Meanwhile, the distribution area of the fuel–air mixture diffuses spatially, and the total amount of combustible mixture increases. The air–fuel ratios around the spark plugs near the intake side and exhaust side gradually become thicker. However, with the advance of the injection timings, a small portion of the fuel–air mixture will inevitably be swept into the exhaust port.

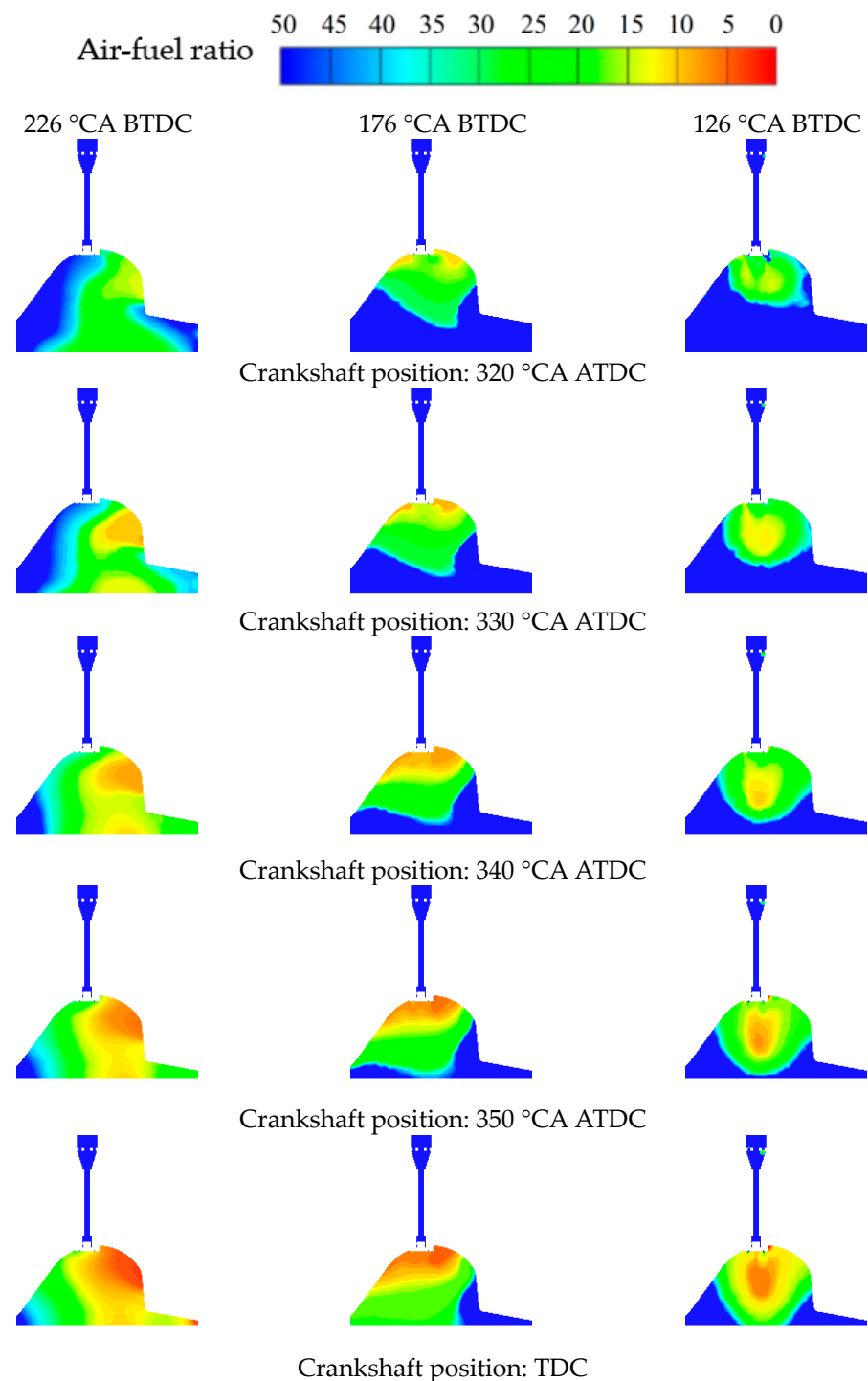


Figure 8. Distribution of mixture concentration in-cylinder at different injection timings.

Figure 9 shows the relationship between the overall SMD of the fuel atomization droplets and the injection timing at different crankshaft positions. From the figure, it can be observed that, with the crankshaft position near the TDC, the overall SMD of the fuel atomization droplets gradually decreases. The main reason is that the air in the combustion chamber and the engine cylinder above the piston is compressed gradually, and the temperature in the cylinder increases. The scavenging airflow in the engine cylinder drives the fuel droplets into continuous motion, which is helpful for the evaporation of the fuel droplets, making the overall SMD smaller. As the injection timing is 226 °CA BTDC and the crankshaft position locates at 340 °CA ATDC, the overall SMD of the fuel droplets

in-cylinder is $11.69 \mu\text{m}$. This indicates that the AADI can maintain a favorable atomization effect on the fuel spray. With the delaying of the injection timing, the overall SMD of the fuel droplets increases significantly due to the shorter evaporation time and increased ambient pressure. As the injection timing is 126°CA BTDC at the crankshaft position of 340°CA ATDC , the overall SMD of the fuel droplets in the cylinder is $47.23 \mu\text{m}$, showing a less combustible mixture. This is not conducive to forming a favorable ignition conditions in the engine combustion chamber.

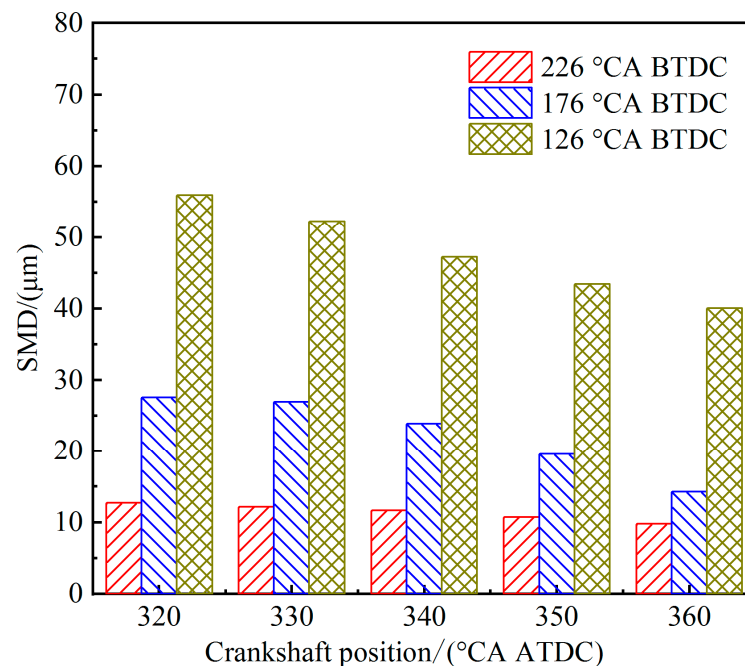


Figure 9. Atomization size of fuel droplets in-cylinder at different injection timings.

3.2. Effects of Injection Pressure on Fuel Atomization and Mixture Formation

To investigate the effects of injection pressure on the fuel atomization characteristics and mixture concentration distribution in-cylinder, the simulation results with different injection pressures are calculated and analyzed under the conditions that the injection timing is 126°CA BTDC , and the fuel temperature is 293 K . Figure 10 shows the fuel–air mixture concentration distribution at the injection pressures of 5.5 bar , 6.5 bar , and 7.5 bar at the engine speed of 4000 r/min . With the increase in injection pressure, the fuel–air mixture is more uniform. As the injection pressure is 5.5 bar , the differential pressure between the outlet of the direct injector and the engine cylinder is small. This is not conducive to the expansion of the spray. Therefore, most fuel droplets are gathered at the top of the combustion chamber, and the distribution area of fuel–air mixture is also quite limited. As the crankshaft position is 340°CA ATDC , the overall amount of fuel evaporated around spark plug near the exhaust side is less, and the air–fuel ratio is about 19.8 . The ignitable condition for the fuel–air mixture is poor. Meanwhile, with the increase in the injection pressure, the distribution area of the fuel–air mixture in-cylinder gradually increases. As the injection pressure is 6.5 bar and the crankshaft position locates at 340°CA ATDC , the air–fuel ratios around the spark plugs near the intake side and exhaust side are about 13.2 , making the fuel–air mixture more easily ignited. In addition, for different engine crankshaft positions, the distribution of the fuel–air mixture formed at the injection pressure of 7.5 bar is more uniform than that formed at the injection pressure of 6.5 bar . As the crankshaft positions are 330°CA ATDC , 340°CA ATDC , and 350°CA ATDC , respectively, the air–fuel ratio around the spark plugs near the intake side and the exhaust side is about 10.3 , which is quite helpful to flame propagation and the expansion of the combustion area in the engine combustion chamber.

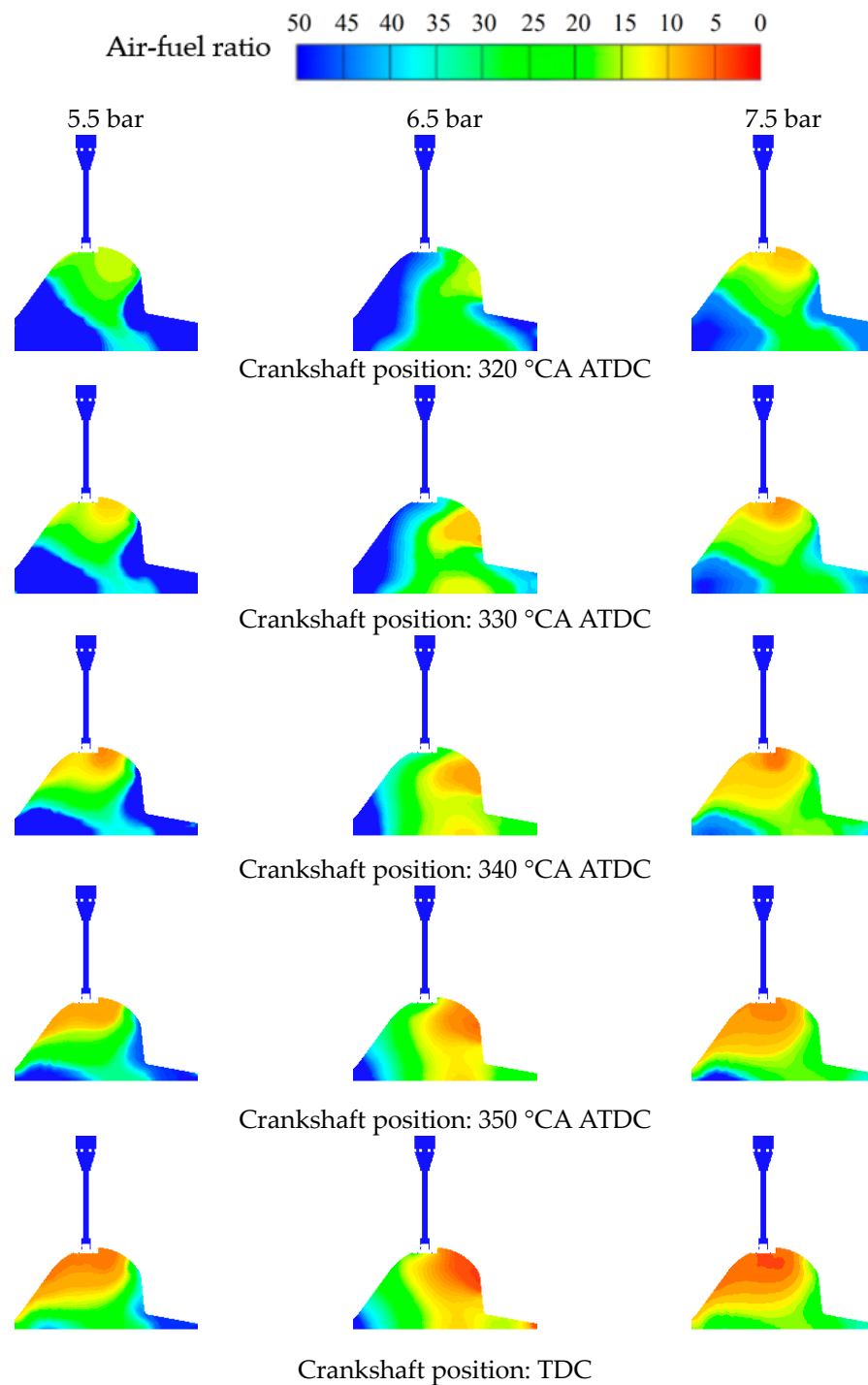


Figure 10. Distribution of mixture concentration in-cylinder at different injection pressures.

Figure 11 shows the relationship between the overall SMD of the fuel spray droplets and the injection pressure at different crankshaft positions. It can be seen from this figure that with the increase in injection pressure, the overall SMD of the fuel droplets decreases. At the crankshaft position of 340 °CA ATDC, the overall SMD of the fuel droplets in the engine cylinder is 14.26 μm as the injection pressure is 5.5 bar. Increasing the injection pressures will easily reduce the overall SMD of the fuel droplets, which indicates the universality of the air-assisted injector for fuel. At the crankshaft position of 340 °CA ATDC, as the injection pressure is 6.5 bar, the overall SMD of the fuel droplets is 11.69 μm , which is 18.1% lower than that at 5.5 bar. Moreover, when the injection pressures are 6.5 bar and 7.5 bar, respectively, the difference of the overall SMD is gradually reduced

as the crankshaft position approaches TDC. However, excessive injection pressure means that more compressed air is consumed, and the power-to-mass ratio of the engine will be reduced. Therefore, under the conditions of reasonable fuel–air mixture formation and the acceptable SMD of fuel droplets, the injection pressure would be as appropriate as possible. As the injection pressure is kept at a level higher than 6.5 bar, the favorable fuel atomization effect in the cylinder can be guaranteed, and the consumption of compressed air in a single cycle can be reduced.

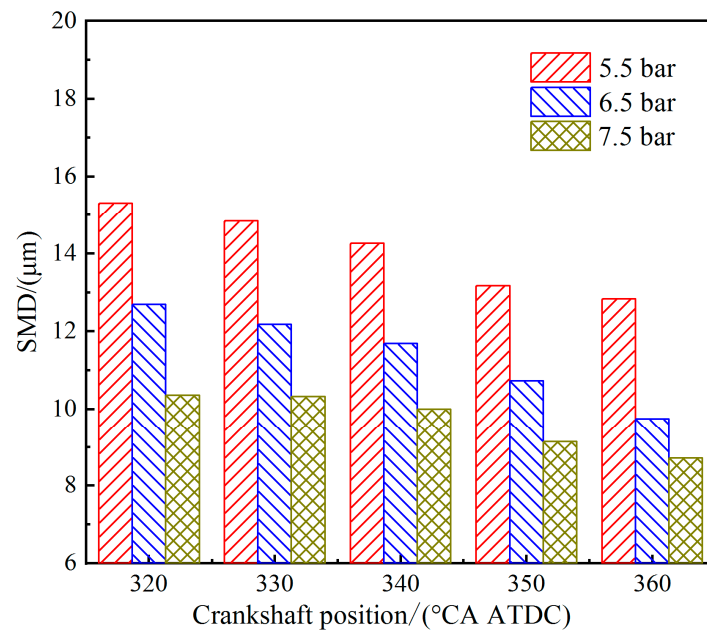


Figure 11. Atomization size of fuel droplets in-cylinder at different injection pressures.

4. Conclusions

In this study, the numerical simulation method is used to investigate the fuel spray atomization and the in-cylinder fuel–air mixture formation of a two-stroke AADI HFE under partial load conditions at an engine speed of 4000 r/min. The effects of injection timing and injection pressure on the atomization of heavy fuel and the concentration distribution of the fuel–air mixture are analyzed. The main conclusions are as follows:

1. The concentration distribution of a combustible mixture in-cylinder is more uniform and the fuel evaporation mass fraction increases after the injection timing is advanced; early injection timings can make the heavy fuel evaporate with sufficient time; the later the injection timing, the larger the overall SMD of the fuel droplets; in addition, premature injection timings will exacerbate the fuel losses.
2. With the increase in injection pressure, the concentration distribution of the combustible mixture in-cylinder is more uniform, which is conducive to the decrease in the overall SMD of the fuel droplets and the propagation of the flame in the cylinder; as the air injection pressures change from 6.5 bar to 7.5 bar, the variations in fuel particle size are small, and the fuel atomization effect remains at a favorable level.
3. This research provides an improved simulation model for heavy fuel spray atomization and mixture formation. The results can provide theoretical support for the optimization of the fuel injection parameters of two-stroke DISI HFEs. Due to the limitation of time and conditions, this research did not carry out detailed bench test research under different injection pressures and injection timings, which should be tested and verified in subsequent research work. This study hopes to contribute to the development of fuel injection control technology for small unmanned vehicles, drones, and all-terrain vehicles.

Author Contributions: Conceptualization, R.L.; data curation, Y.Q., H.J., L.Z., and H.W.; formal analysis, R.L. and H.J.; funding acquisition, R.L. and K.H.; investigation, R.L. and Y.Q.; project administration, K.H.; resources, R.L.; software, Y.Q., L.Z., and H.W.; supervision, K.H.; writing—original draft, R.L.; writing—review and editing, R.L. and K.H. All authors have read and agreed to the published version of the manuscript.

Funding: This work was supported by the National Key Research and Development Program of China (Grant No. 2018YFE0117500); the National Natural Science Foundation of China (Grant No. 51865031); the State Key Laboratory of Engines, Tianjin University (Grant No. K2020-05); and the Natural Science Foundation of the Jiangsu Higher Education Institutions of China (Grant No. 20KJB470014).

Institutional Review Board Statement: Not applicable.

Informed Consent Statement: Not applicable.

Data Availability Statement: All data used to support the findings of this study are included within the article.

Acknowledgments: This research project was generously supported by the Jiangsu Province Key Laboratory of Aerospace Power Systems.

Conflicts of Interest: The authors declare no conflict of interest.

References

1. Wang, C.; Lu, J.; Ren, Z.; Wan, Z.; Zhao, Z. Current development state and investigation of application for small piston aero-engine. In Proceedings of the 9th Youth Science and Technology Forum of Chinese Aeronautical Society, Xian, China, 17 November 2020; pp. 324–330.
2. Lu, D.; Zheng, J.; Hu, C. Study on the development status of general aviation piston engine. *Intern. Combust. Engines Parts* **2019**, *10*, 64–66.
3. Xu, J.; Nie, K.; Huang, G.; Sheng, Y. Control of torque and air-fuel ratio of compression-ignition aero piston engine. *J. Aerosp. Power* **2021**, *36*, 1083–1093.
4. Du, C.; Tian, M.; Hu, C. Technical development analysis of two-stroke heavy fuel aero engine. *Small Intern. Combust. Engine Veh. Technol.* **2020**, *49*, 92–96.
5. Liu, R.; Wei, M.; Yang, H. Cold start control strategy for a two-stroke spark ignition diesel-fuelled engine with air-assisted direct injection. *Appl. Therm. Eng.* **2016**, *108*, 414–426. [[CrossRef](#)]
6. Wei, M.; Liu, R.; Yang, H.; Bei, T.; Ji, H.; Chang, C. Partial load experiments on a two-stroke spark ignition direct injection heavy fuel engine. *J. Aerosp. Power* **2017**, *32*, 2919–2926.
7. Queiroz, C.; Tomanik, E. *Gasoline Direct Injection Engines—A Bibliographical Review*; SAE Technical Paper 973113; SAE International: Warrendale, PA, USA, 1997.
8. Li, C. Study on the Mixture Formation and Combustion of Light-Weight High-Speed Heavy Oil Aeroengine. Master's Thesis, Beijing Jiaotong University, Beijing, China, 2014.
9. Hu, C.M.; Wang, S.D.; Bi, Y.F.; Zhong, W.J. Combustion characteristics of direct injection piston aviation kerosene engine. *J. Aerosp. Power* **2017**, *32*, 1035–1042.
10. Chen, Z.; Qin, T.; He, T.; Zhu, L. Effect of equivalence ratio on diesel direct injection spark ignition combustion. *J. Cent. South Univ.* **2020**, *27*, 2338–2352. [[CrossRef](#)]
11. Chen, Z.; Liao, B.; Yu, Y.; Qin, T. Effect of equivalence ratio on spark ignition combustion of an air-assisted direct injection heavy-fuel two-stroke engine. *Fuel* **2022**, *313*, 122646. [[CrossRef](#)]
12. Zhao, Z.; Yu, C.; Dong, X.; Wang, L. Research on mixture formation of two-stroke heavy fuel direct injection engine. *J. Aerosp. Power* **2021**, *36*, 1569–1577.
13. Huang, L. CFD Simulation Study of the Fuel-Air Mixture Formation in Cylinder of the Two-stroke Heavy Fuel Spark Ignition Engine. Master's Thesis, Nanjing University of Aeronautics and Astronautics, Nanjing, China, 2016.
14. Wang, S. Research on GDI Technology of Small Model Two-Stroke Kerosene Engine. Master's Thesis, Nanjing University of Aeronautics and Astronautics, Nanjing, China, 2017.
15. Wang, S.; Yang, H. Simulation on Atomization Mechanism of Air-Assisted Injector for Aircraft Heavy Fuel Engine. *Trans. CSICE* **2018**, *36*, 127–135.
16. Ji, H.; Wu, H.; Yang, H.; Liu, H.; Rui, L. Numerical simulation of diesel spray characteristics based on air-assisted atomization injection. *J. Aerosp. Power* **2022**, *37*, 1284–1294.
17. Shih, T.-H.; Liou, W.; Shabbir, A.; Yang, Z.; Zhu, J. A new k- ϵ eddy viscosity model for high reynolds number turbulent flows. *Comput. Fluids* **1995**, *24*, 227–238. [[CrossRef](#)]
18. O'Rourke, P. *The TAB Method for Numerical Calculation of Spray Droplet Breakup*; SAE Technical Paper 872089; SAE International: Warrendale, PA, USA, 1987.

19. ANSYS, Inc. *ANSYS Fluent Theory Guide 19.1*; ANSYS, Inc.: Canonsburg, PA, USA, 2018; pp. 195–197.
20. Han, Z.; Fan, L.; Reitz, R.D. *Multidimensional Modeling of Spray Atomization and Air-Fuel Mixing in a Direct-Injection Spark-Ignition Engine*; SAE Transactions: Warrendale, PA, USA, 1997; pp. 1423–1441.
21. GB 19147-2016[S/OL]; Automobile Diesel Fuels. National Technical Committee on Petroleum Products and Lubricants of Standardization Administration of China, Standards Press of China: Beijing, China, 23 December 2016.
22. Liu, R.; Ji, H.; Wei, M. Study of low load performance on a two-stroke direct injection spark ignition aero-piston engine fuelled with diesel. *Aircr. Eng. Aerosp. Technol.* **2021**, *93*, 473–482. [[CrossRef](#)]
23. Ma, Y.; Haiqing, Y.; Xu, G. Numerical simulation of stratified scavenging two-stroke gasoline engine. *J. Aerosp. Power* **2019**, *34*, 2001–2009.
24. Li, Z.; Hua, J.; Wei, H.; Zhang, L. Experimental and 1-D Simulation Studies of Gasoline Direct Ignition Engine. *J. Combust. Sci. Technol.* **2018**, *24*, 238–244.
25. Bei, T.; Wei, M.; Liu, R.; Sheng, J. Effects of asynchronous ignition phase on knock combustion of two-stroke engine. *J. Aerosp. Power* **2017**, *32*, 322–329.